Supplementary Information

Heat-guided drug delivery via thermally induced crosslinking of polymeric micelles

Sota Yamada, Eita Sasaki, Hisashi Ohno, and Kenjiro Hanaoka*

Faculty of Pharmacy and Graduate School of Pharmaceutical Sciences, Keio University, Tokyo 105-8512, Japan

*Corresponding author e-mail: khanaoka@keio.jp

Table of Contents

Scheme S1. Synthesis of DBCO-P(NIPAAm-*co*-AAm)-*b*-PBMA

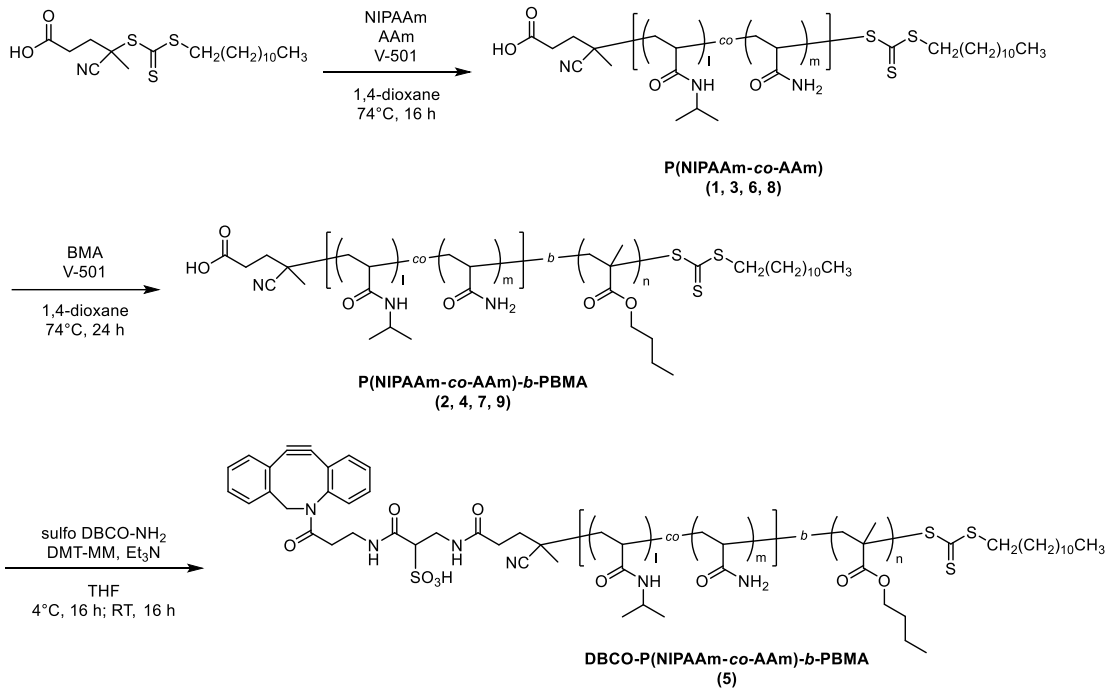

Scheme S2. Synthesis of P(Az-*co*-AAm)-*b*-PBMA

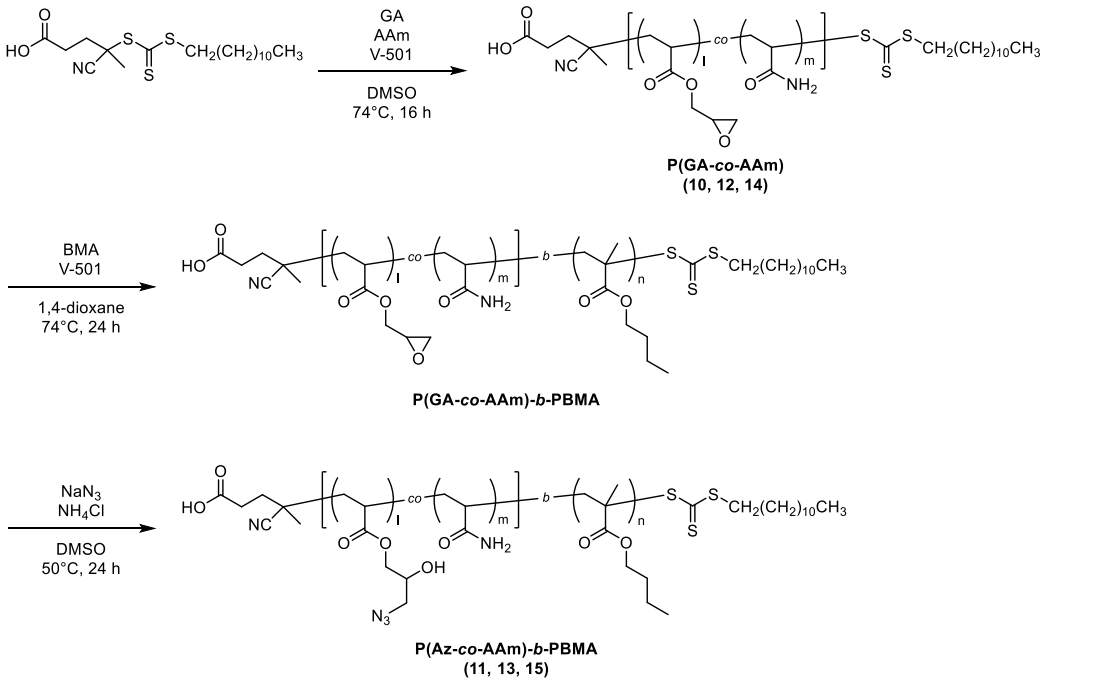

Table S1. Characterization of the polymers.

	Polymer	Molar ratio (in feed)			Molar ratio (in polymer) [a]			[monomer] / [CTA]	*M*n (GPC) [b]	*M*n (NMR)	PDI [e]
		NIPAAm	AAm	GA	NIPAAm	AAm	Az				
(i) Polymers for preparation of DBCO-TRM											
1	P(NIPAAm-*co*-AAm4)	96	4	0	96	4	0	80	8600	–	1.16
2	P(NIPAAm-*co*-AAm4)-*b*-PBMA	–	–	–	96	4	0	50	9300	11000 [c]	1.19
3	P(NIPAAm-*co*-AAm16)_long	84	16	0	84	16	0	120	11800	–	1.13
4	P(NIPAAm-*co*-AAm16)_long-*b*-PBMA	–	–	–	84	16	0	50	13300	14100 [c]	1.22
5	DBCO-P(NIPAAm-*co*-AAm16)-*b*-PBMA	–	–	–	84	16	0	–	–	–	–
(ii) Polymers for preparation of DBCO-TRM(high)											
6	P(NIPAAm-*co*-AAm16)	84	16	0	84	16	0	80	8300	–	1.17
7	P(NIPAAm-*co*-AAm16)-*b*-PBMA	–	–	–	84	16	0	50	9300	12700 [c]	1.24
(iii) Polymers for preparation of Az-TRM											
8	P(NIPAAm-*co*-AAm8)	92	8	0	92	8	0	140	14000	–	1.15
9	P(NIPAAm-*co*-AAm8)-*b*-PBMA	–	–	–	92	8	0	50	14800	17700 [c]	1.18
10	P(GA-*co*-AAm)	0	70	30	–	–	–	110	6800	16700 [d]	1.15
11	P(Az-*co*-AAm)-*b*-PBMA	–	–	–	0	73	27	50	20100	–	1.74
(iv) Polymers for preparation of Az-TRM(short)											
12	P(GA-*co*-AAm)_short	0	70	30	–	–	–	60	5700	11000 [d]	1.21
13	P(Az-*co*-AAm)_short-*b*-PBMA	–	–	–	0	73	27	50	13700	–	1.43
(v) Polymers for preparation of Az-TRM(long)											
14	P(GA-*co*-AAm)_long	0	70	30	–	–	–	200	8500	23300 [d]	1.25
15	P(Az-*co*-AAm)_long-*b*-PBMA	–	–	–	0	72	28	50	26800	–	1.92

[a] Calculated from the ^{1}H NMR spectra. [b] Determined by GPC. Number-average molecular weight (*M*n), weight-average molecular weight (*M*w). [c] Calculated by ^{1}H NMR using the *M*n of the first block polymer. [d] Calculated by ^{1}H NMR using the *M*n of the diblock polymer determined by GPC. Since the ratio of the monomer to the chain transfer agent in the second step was lower than that in the first step, we considered that the molecular weights of the first block might not have been correctly measured by GPC. [e] PDI is the polydispersity index of the weight distribution, calculated as *M*w/*M*n.

Table S2. Characterization of the micelles

Micelle	Polymer (wt%)		Mean diameter (nm) [a]	PDI [a]	CMC (μg/mL) [b]	LCST (°C) [c]
DBCO-TRM	P(NIPAAm-*co*-AAm4)-*b*-PBMA (2)	70	119 ± 1.4	0.148 ± 0.009	4.7	39.6
	DBCO-P(NIPAAm-*co*-AAm16)-*b*-PBMA (5)	30				
Az-TRM	P(NIPAAm-*co*-AAm8)-*b*-PBMA (9)	90	114 ± 1.6	0.208 ± 0.017	3.0	39.7
	P(AAm-*co*-Az)-*b*-PBMA (11)	10				
TRM	P(NIPAAm-*co*-Aam8)-*b*-PBMA (9)	100	110 ± 2.0	0.186 ± 0.019	1.7	39.4
DBCO-TRM(high)	P(NIPAAm-*co*-AAm16)-*b*-PBMA (7)	70	110 ± 0.1	0.138 ± 0.009	–	52.3
	DBCO-P(NIPAAm-*co*-AAm16)-*b*-PBMA (5)	30				
Az-TRM(short)	P(NIPAAm-*co*-AAm8)-*b*-PBMA (9)	90	130 ± 3.2	0.170 ± 0.036	–	39.5
	P(AAm-*co*-Az)_short-*b*-PBMA (13)	10				
Az-TRM(long)	P(NIPAAm-*co*-AAm8)-*b*-PBMA (9)	90	124 ± 0.8	0.253 ± 0.007	–	39.8
	P(AAm-*co*-Az)_long-*b*-PBMA (15)	10				
DBCO-TRM@Dox	P(NIPAAm-*co*-AAm4)-*b*-PBMA (2)	70	113 ± 0.8	0.132 ± 0.010	4.7	39.5
	DBCO-P(NIPAAm-*co*-AAm16)-*b*-PBMA (5)	30				

[a] Measured by dynamic light scattering at 25°C in PBS. PDI is the polydispersity index of the particle size distribution. [b] Determined using pyrene as a fluorescent probe. [c] Determined from the optical transmittance changes.

Table S3. Reaction ratio of DBCO-TRM and Az-TRM

	DBCO-TRM	Az-TRM	Reaction ratio
Combination in Figure 3b	DiI-loaded	DiD-loaded	1.00 ± 0.05
Combination in Figure S3	DiD-loaded	DiI-loaded	1.03 ± 0.11

DBCO-TRM and Az-TRM were mixed equally (1.0 mg/mL in PBS) and heated twice at 42°C for 10 min. After centrifugation at 25°C, the precipitates were dissolved with DMSO and the reaction ratio of DBCO-TRM to Az-TRM was calculated from the fluorescence intensity of DiI and DiD (mean ± SD, n = 3).

Table S4. Effect of the mixing ratio of DBCO-TRM and Az-TRM on the aggregates

Mixing ratio (DBCO-TRM / Az-TRM)	0.33	1.00	3.00
Reaction ratio (DBCO-TRM / Az-TRM)	0.31 ± 0.01	1.04 ± 0.02	2.65 ± 0.06

DiI-loaded DBCO-TRM (1.0 mg/mL in PBS) and DiD-loaded Az-TRM (1.0 mg/mL in PBS) were mixed at the indicated ratio and heated twice at 42°C for 10 min. After centrifugation at 25°C, the precipitates were dissolved in DMSO and the reaction ratio of DBCO-TRM to Az-TRM was calculated from the fluorescence intensity of DiI and DiD (mean ± SD, n = 4).

Table S5. Serum biochemical levels of tumor-bearing mice at 48 h after the injection.

Groups	ALT (U/L)	AST (U/L)	BUN (mg/L)	CRE (mg/L)	D-dimer (mg/L)
PBS	98 ± 20	45 ± 4.5	182 ± 11	1.30 ± 0.14	1.96 ± 0.44
Dox	108 ± 23	40 ± 14	181 ± 41	1.46 ± 0.05	1.90 ± 0.29
DBCO-TRM@Dox & Az-TRM	111 ± 15	45 ± 4.8	164 ± 17	1.32 ± 0.13	1.95 ± 0.46
DBCO-TRM@Dox & Az-TRM + heating	99 ± 16	44 ± 11	180 ± 19	1.24 ± 0.17	1.89 ± 0.35

All data are the means ± SD (n = 5). All parameters in test groups showed no significant difference from those in the PBS control ($p > 0.05$). ALT: serum alanine aminotransferase; AST: aspartate aminotransferase; BUN: blood urea nitrogen; CRE: creatinine.

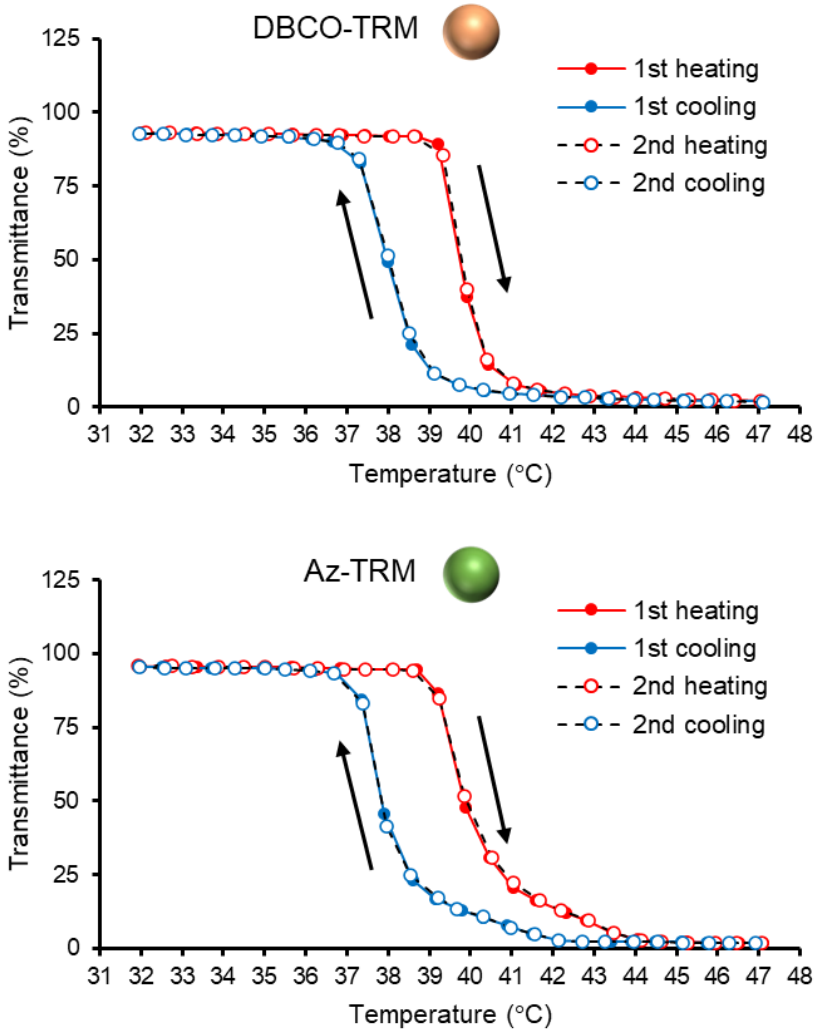

Figure S1. Reversible change of optical transmittance of the micelles. Condition: 1 mg/mL micelle in PBS at a heating/cooling rate of 1.0°C/min.

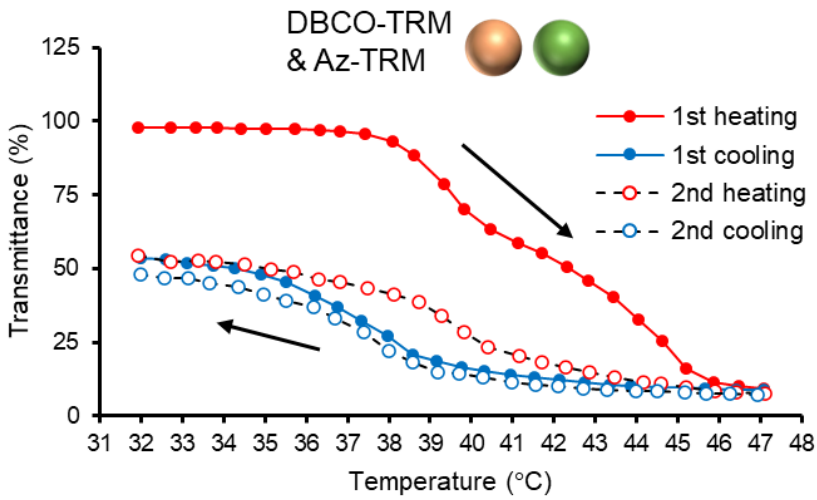

Figure S2. Irreversible change of optical transmittance of the mixture of DBCO-TRM and Az-TRM. Condition: 1 mg/mL micelle in PBS at a heating/cooling rate of 1.0°C/min.

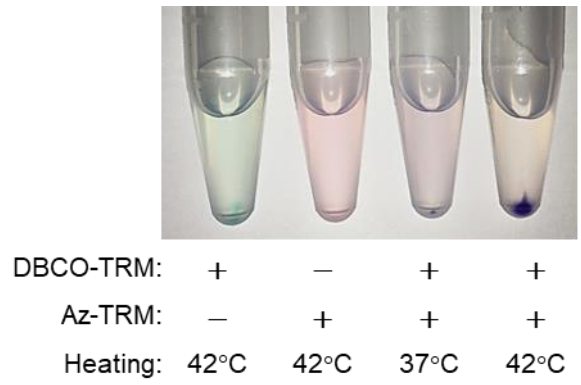

Figure S3. Photographs of micellar aggregates after heating. DiD-loaded DBCO-TRM (colored blue) and DiI-loaded Az-TRM (colored red) were mixed equally (1.0 mg/mL in PBS). After heating twice at the indicated temperature for 10 min, the micelle mixture was centrifuged at 25°C.

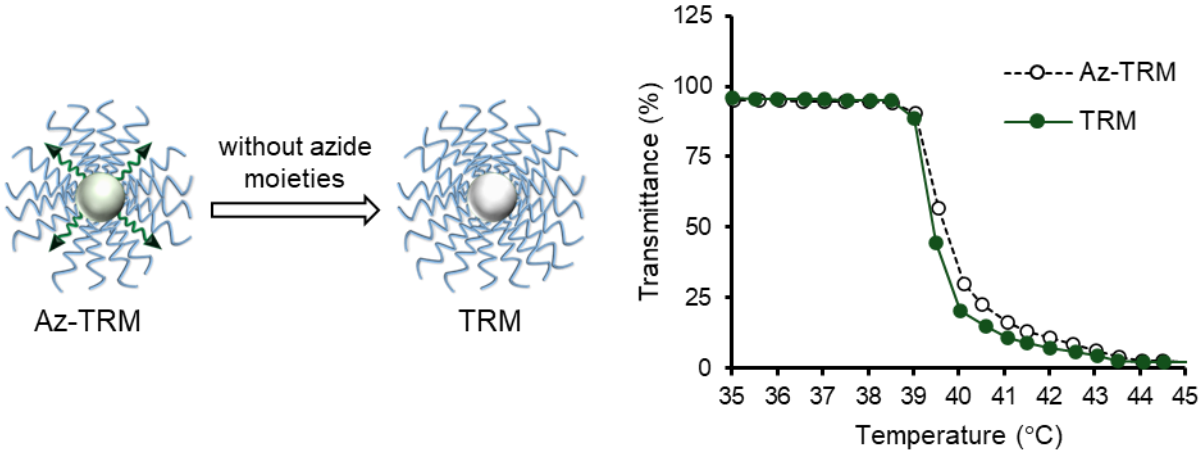

Figure S4. Illustration of TRM and the temperature responsiveness. TRM was prepared from P(NIPAAm-*co*-AAm)-*b*-PBMA without any azide-containing polymer.

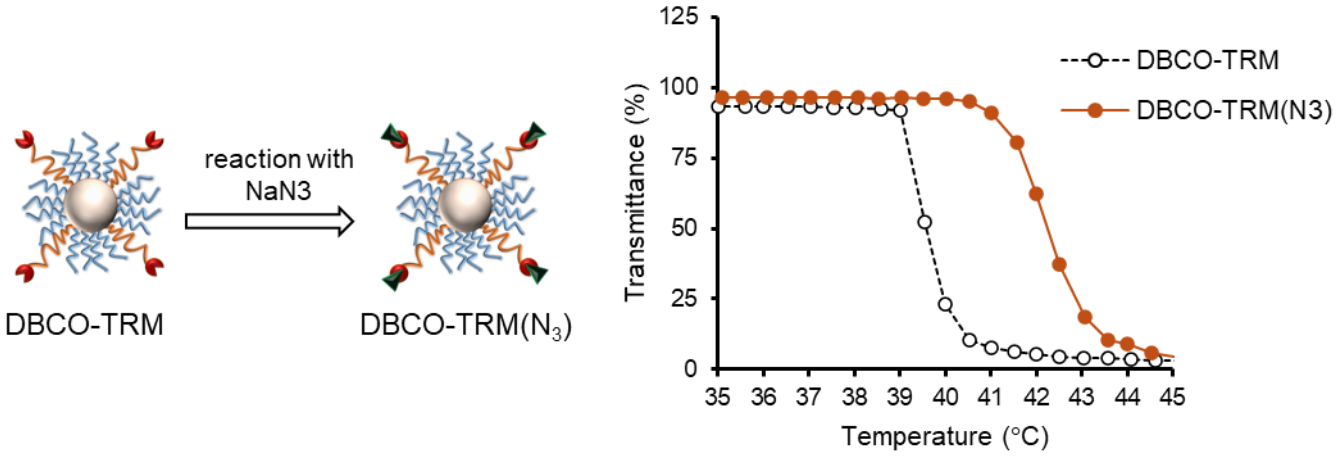

Figure S5. Illustration of DBCO-TRM(N_3) and the temperature responsiveness. DBCO-TRM was reacted with 0.1 ccccccwt% NaN_3 in PBS for 30 min at room temperature to deactivate DBCO.

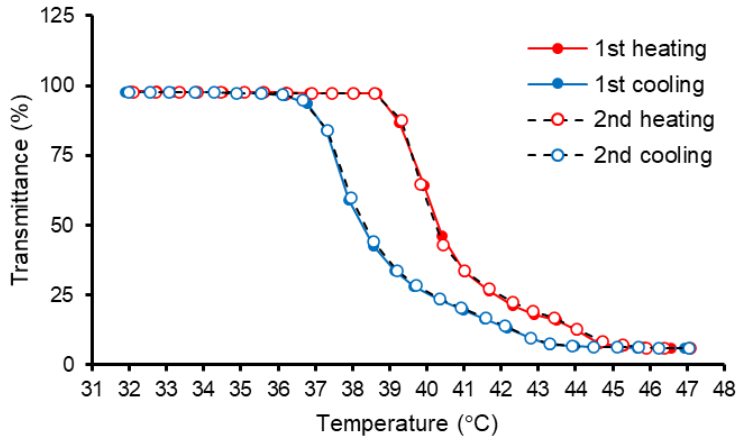

Figure S6. Reversible change of optical transmittance of the mixture of DBCO-TRM and TRM. Condition: 1 mg/mL micelles in PBS at a heating/cooling rate of 1.0°C/min.

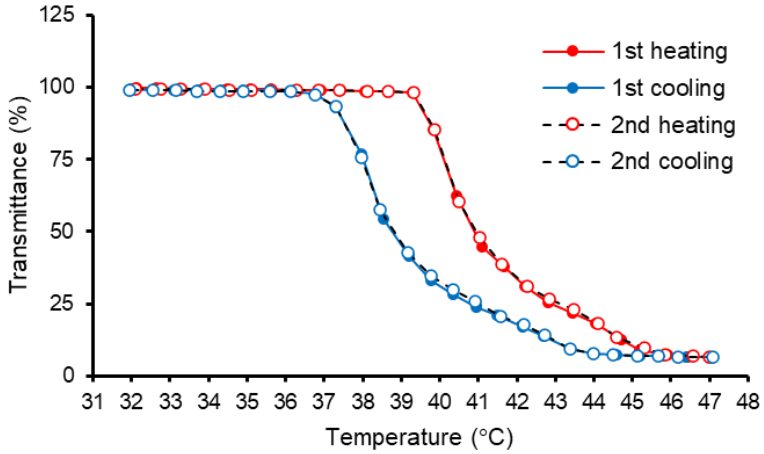

Figure S7. Reversible change of optical transmittance of the mixture of DBCO-TRM(N_3) and Az-TRM. Condition: 1 mg/mL micelles in PBS at a heating/cooling rate of 1.0°C/min.

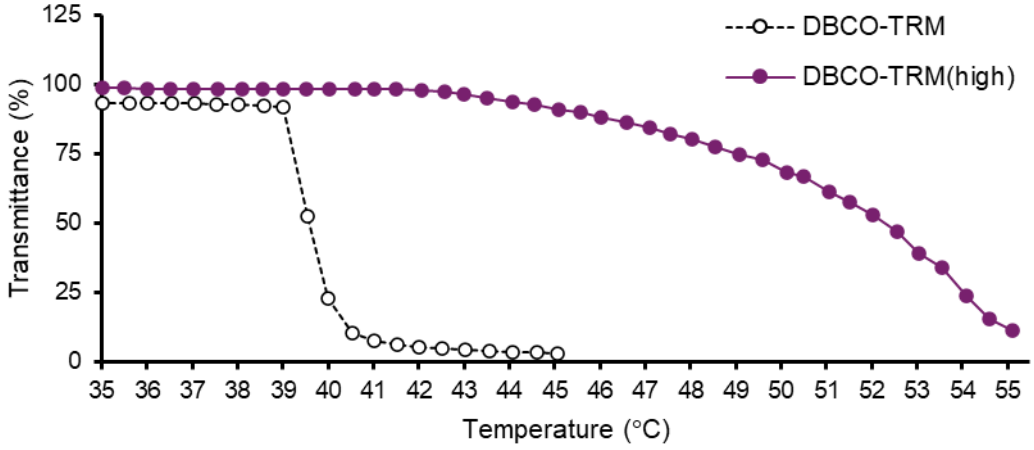

Figure S8. Temperature-dependent change of optical transmittance of DBCO-TRM(high). Condition: 1 mg/mL micelles in PBS.

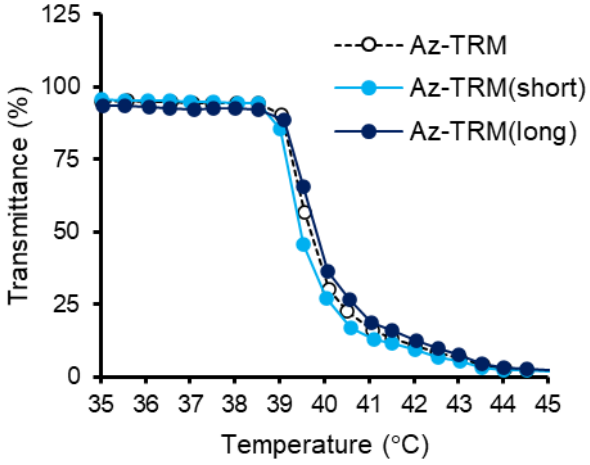

Figure S9. Temperature-dependent change of optical transmittance of Az-TRM(short) and Az-TRM(long). Condition: 1 mg/mL micelles in PBS.

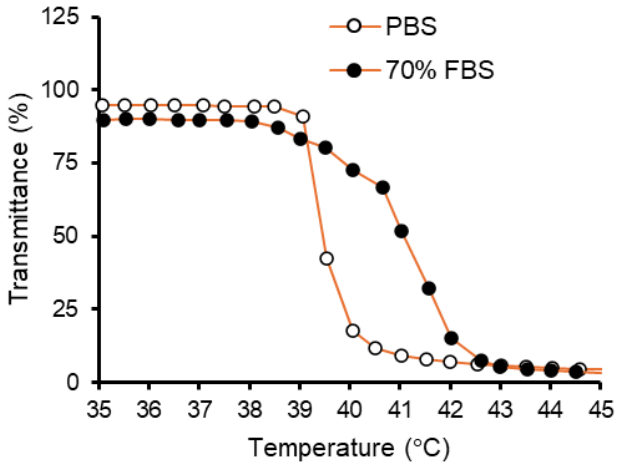

Figure S10. Effect of FBS on the temperature responsiveness of DBCO-TRM (1 mg/mL).

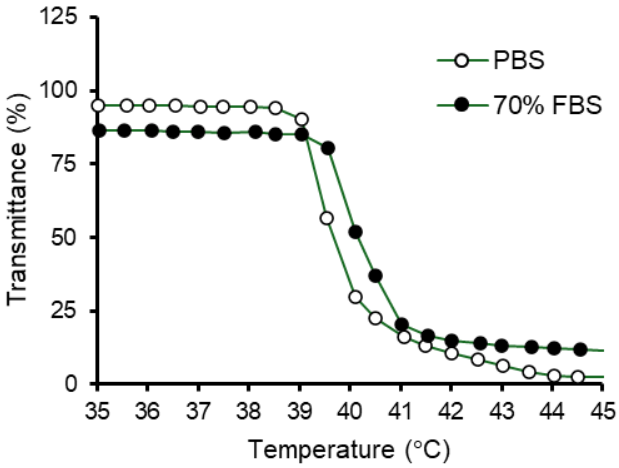

Figure S11. Effect of FBS on the temperature responsiveness of Az-TRM (1 mg/mL).

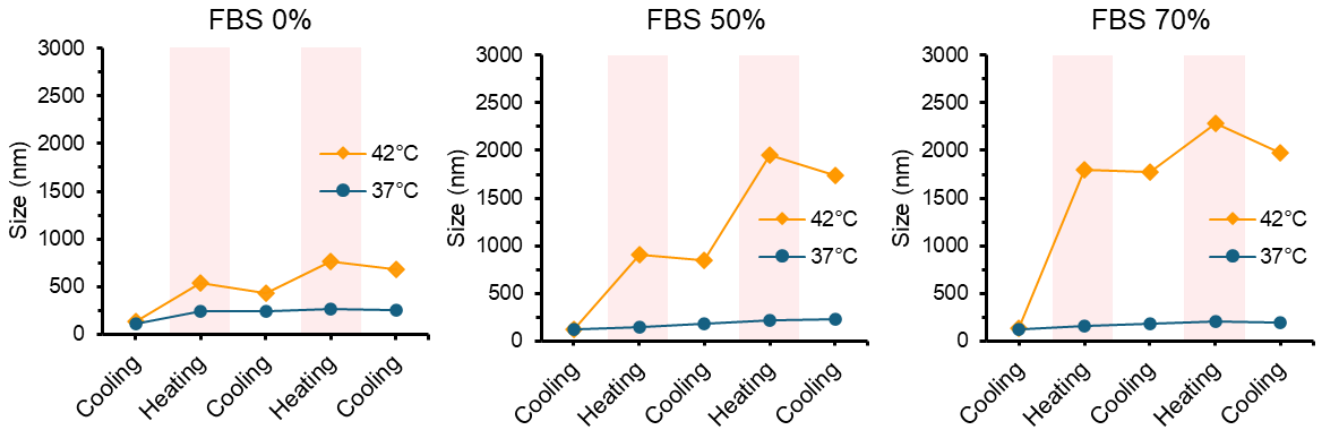

Figure S12. Effect of FBS on the aggregation of DBCO-TRM and Az-TRM. The temperature was cyclically changed between 32°C (cooling) and the indicated temperature (heating), and the size of micelles in the mixture of DBCO-TRM and Az-TRM in PBS containing FBS was measured by DLS after holding the temperature at the indicated value for 5 min.

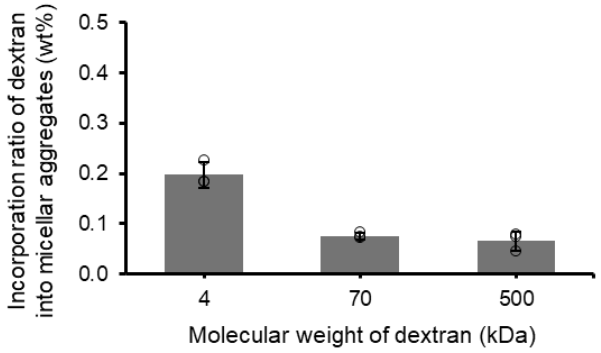

Figure S13. Incorporation of dextran into irreversible aggregates of DBCO-TRM and Az-TRM. FITC-labelled dextran was mixed at the same concentration (1 mg/mL) with DiD-loaded DBCO-TRM and DiD-loaded Az-TRM in PBS and the mixture was heated twice at 42°C for 10 min. After centrifugation at 25°C, the precipitates were dissolved in 90% DMSO and the incorporation ratio of dextran to the aggregates was calculated from the fluorescence intensities of FITC and DiD (mean ± SD, n = 3).

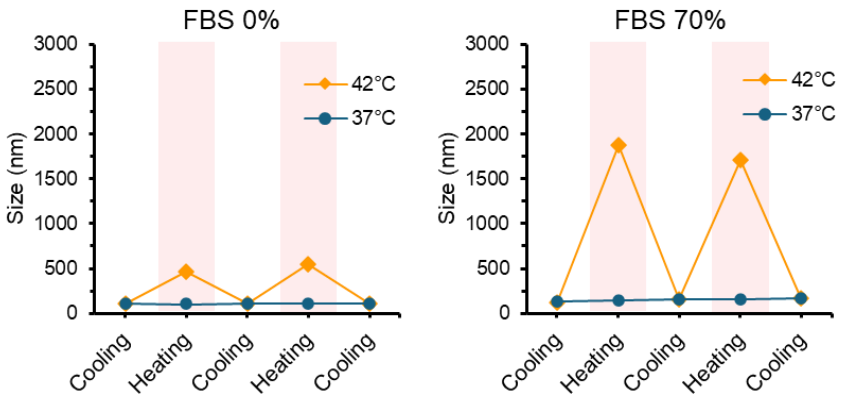

Figure S14. Effect of FBS on the aggregation of DBCO-TRM and TRM (non-azide control). The temperature was cycled between 32°C (cooling) and the indicated temperature (heating), and the size of the micelle mixture was measured by DLS after holding the temperature at the indicated value for 5 min.

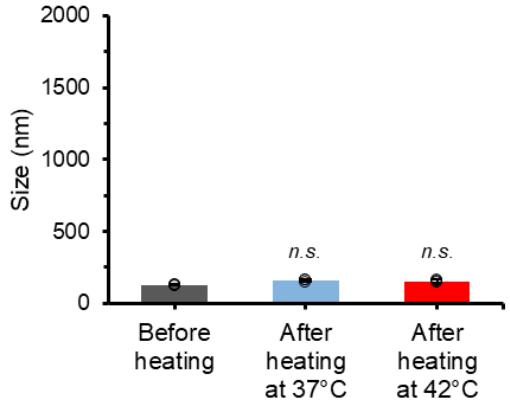

Figure S15. Size of aggregates in a mixture of DBCO-TRM and TRM after heating in the presence of serum. DiI-loaded DBCO-TRM and TRM were mixed in equal amounts (1.0 mg/mL in PBS containing 70% FBS). The mixture was heated twice at the indicated temperature for 10 min, the size of the micelle mixture was measured by DLS at 32°C.

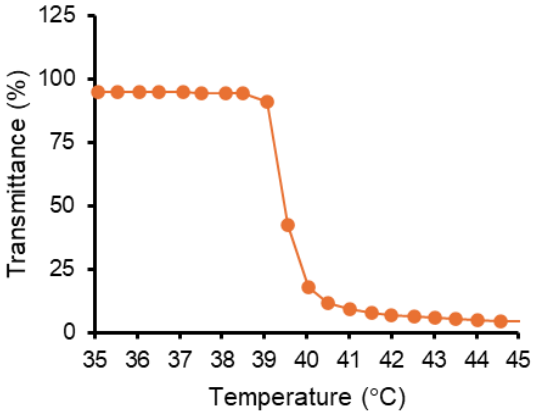

Figure S16. Temperature-dependent change of optical transmittance of DBCO-TRM@Dox. Condition: 1 mg/mL micelles in PBS.

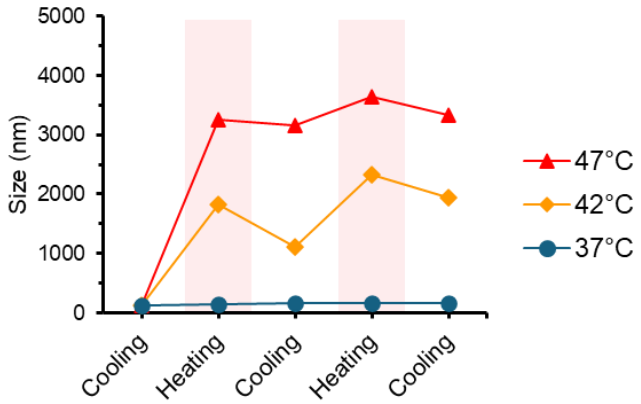

Figure S17. Irreversible response to heating of a mixture of DBCO-TRM@Dox and Az-TRM. The temperature was cyclically changed between 32°C (cooling) and the indicated temperature (heating), and the size of micelles in the mixture of DBCO-TRM@Dox and DiD-loaded Az-TRM in PBS was measured by DLS after holding the temperature at the indicated value for 5 min.

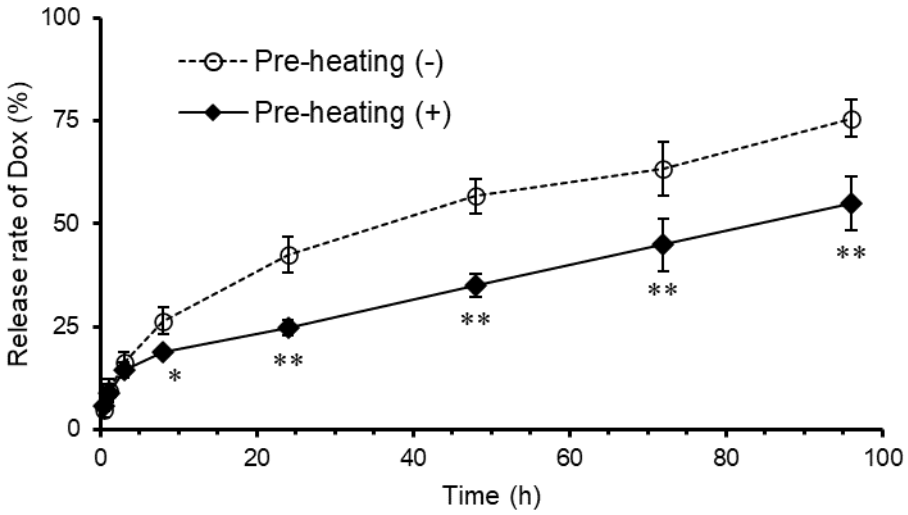

Figure S18. *In vitro* Dox release from aggregates of DBCO-TRM@Dox and Az-TRM. DBCO-TRM@Dox and Az-TRM were mixed equally and pre-heated at 42°C for 10 min twice. The resulting mixture was dialyzed against PBS (pH 7.4) containing 1% Tween-20 at 37°C with continuous shaking at 100 rpm (mean ± SD, $n = 3$). *$p < 0.05$ and **$p < 0.01$ versus Pre-heating (–) (Student's t-test).

Figure S19. Photograph of *in vivo* local heating. Under isoflurane anaesthesia, an electric hand warmer was placed over the tumor site of the mouse. To prevent contact of the warmer with sites other than the tumor, paper was placed between the warmer and the right leg and tail of the mouse.

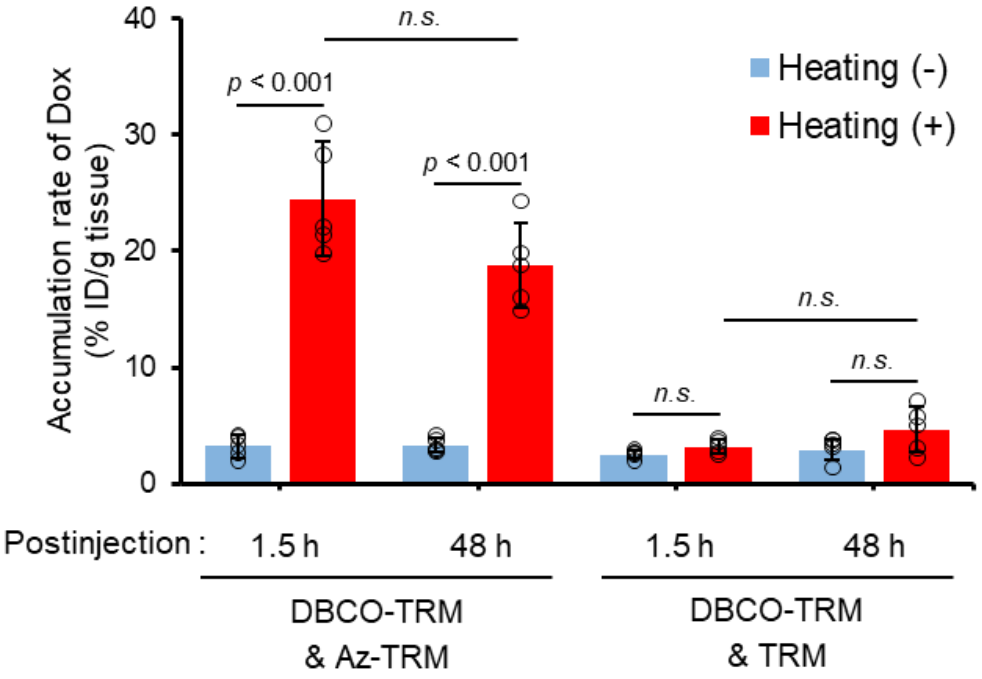

Figure S20. Accumulation of Dox at the tumor site. The accumulation of Dox in the tumor is shown as % ID/g (percentage of injected dose per gram of tissue, calculated from the fluorescence intensity of Dox in tissue lysate) (mean ± SD, n = 5, Student's t-test).

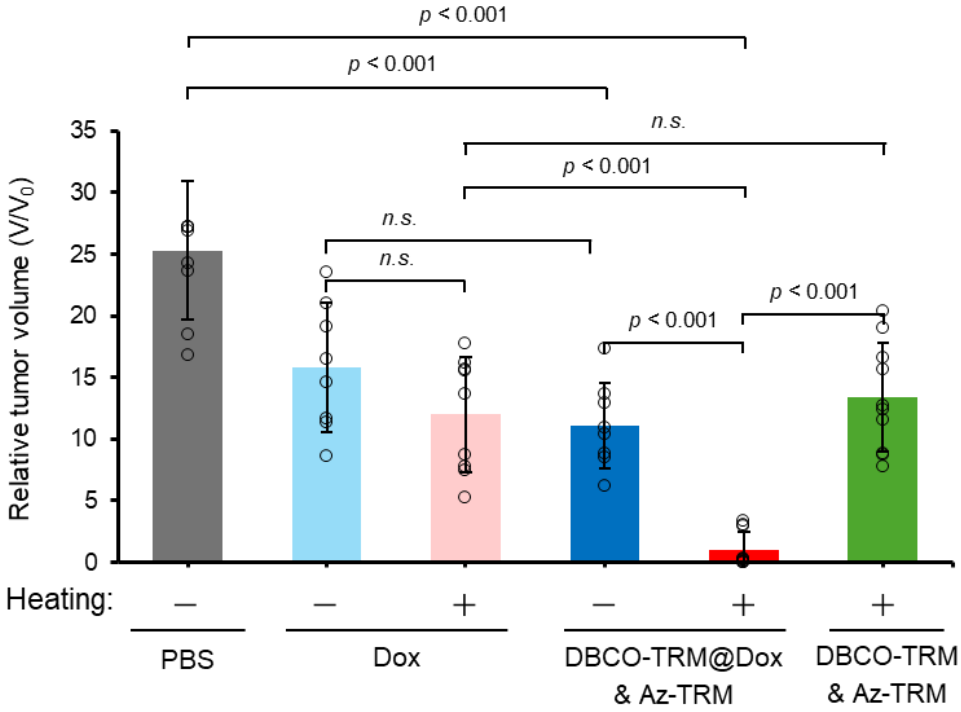

Figure S21. Relative tumor volume on day 18 was calculated as the ratio to the volume on day 0. The significance of differences was analyzed by means of the Mann-Whitney U test (mean ± SD, n = 8–10, Student's t-test).

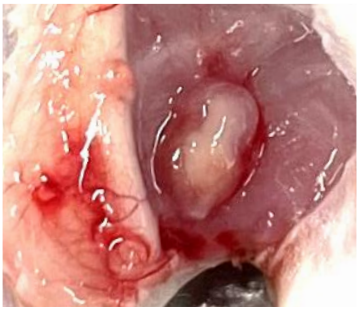

Figure S22. Photograph of the tumor and subcutaneous tissue of mice at 48 h after treatment with DBCO-TRM (without Dox) and Az-TRM with heating.

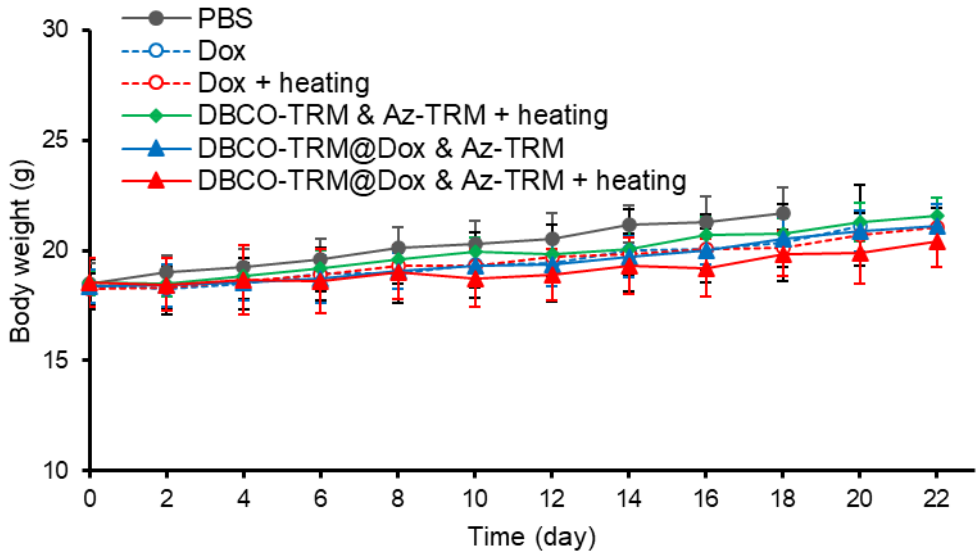

Figure S23. Body weight changes of tumor-beating mice after the different treatments (mean ± SD, n = 8–10).

^{1}H NMR spectra of the polymers

(1) P(NIPAAm-*co*-AAm4) in DMSO-d_6.

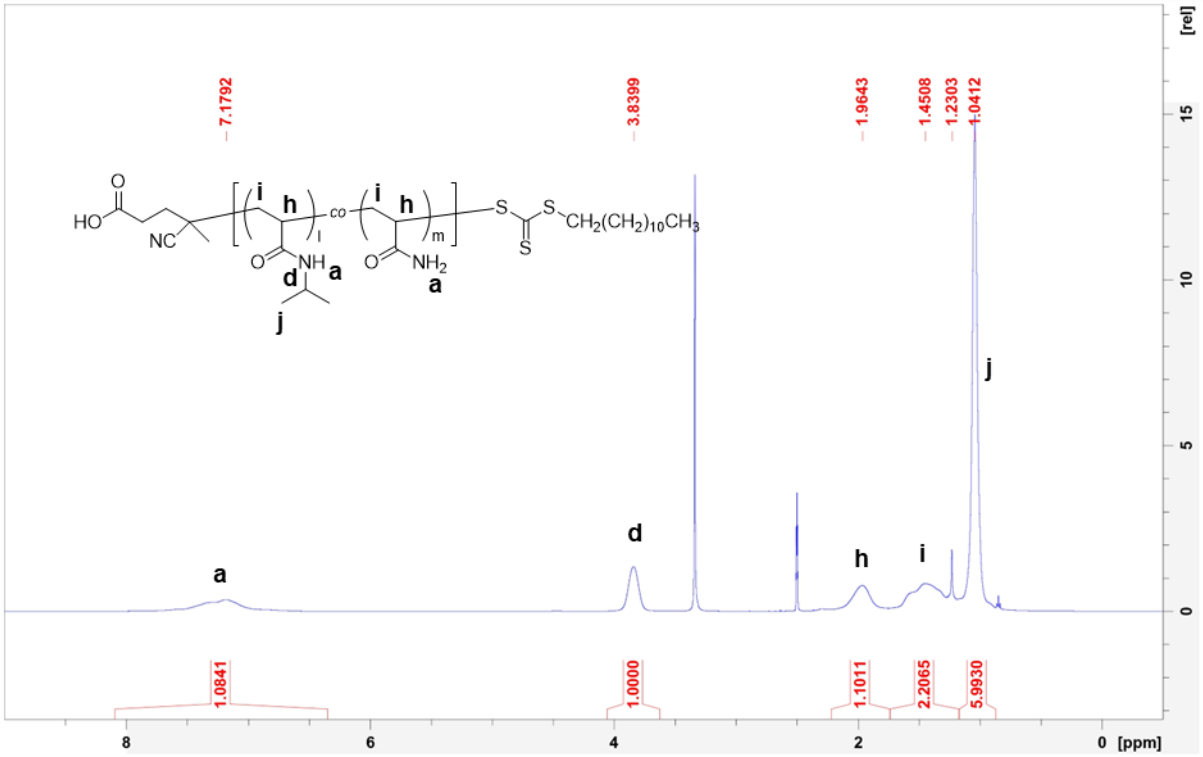

(2) P(NIPAAm-*co*-AAm4)-*b*-PBMA in DMSO-d_6.

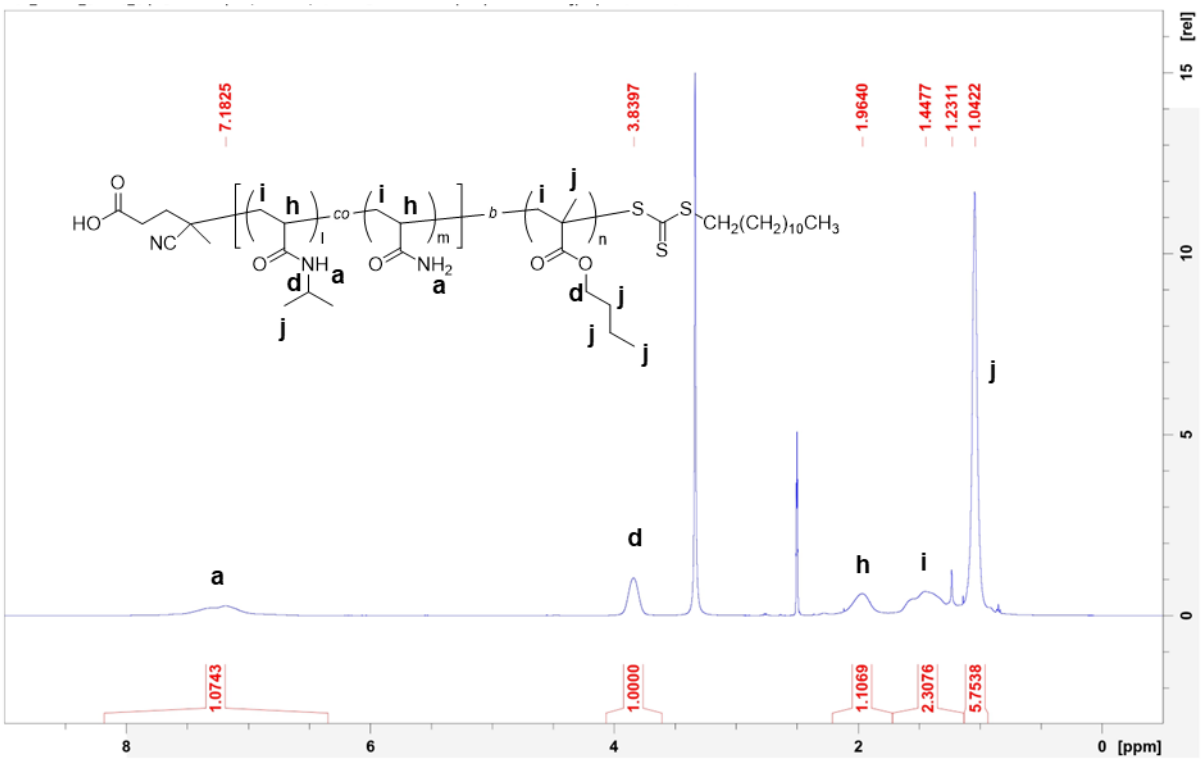

(3) P(NIPAAm-*co*-AAm16)_long in DMSO-d_6.

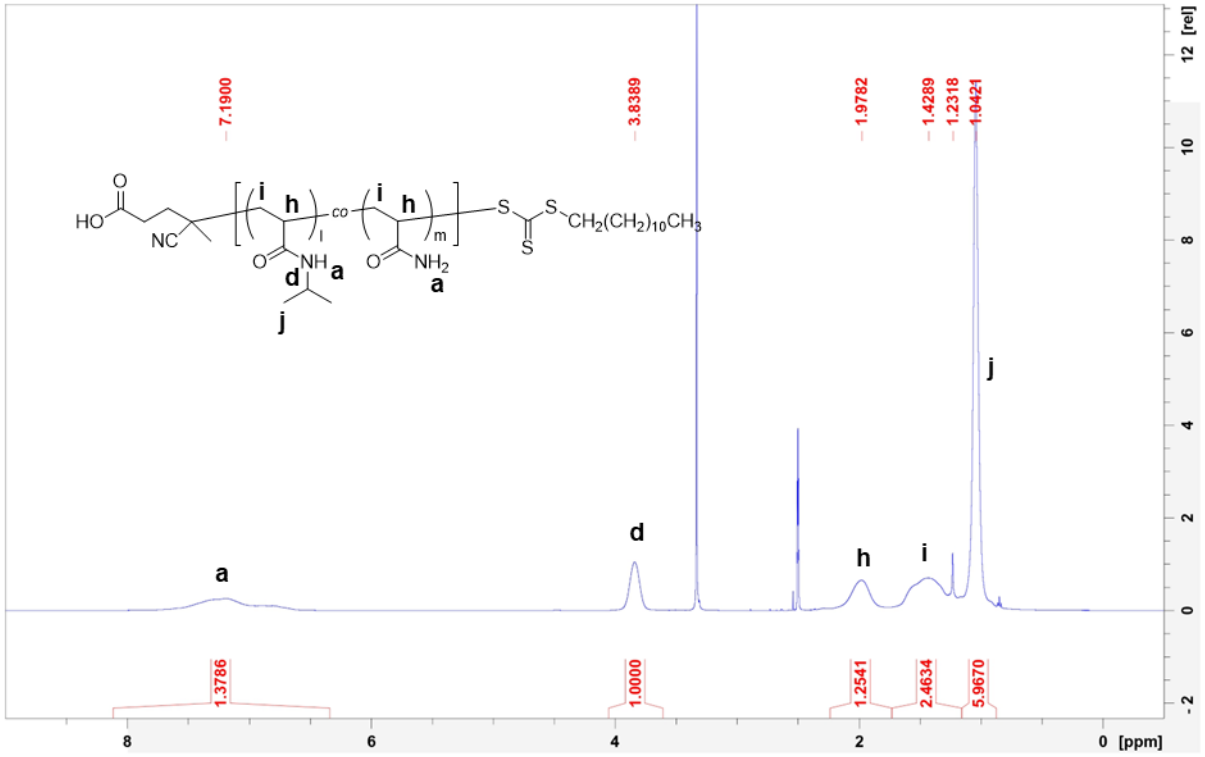

(4) P(NIPAAm-*co*-AAm16)_long-*b*-PBMA in DMSO-d_6.

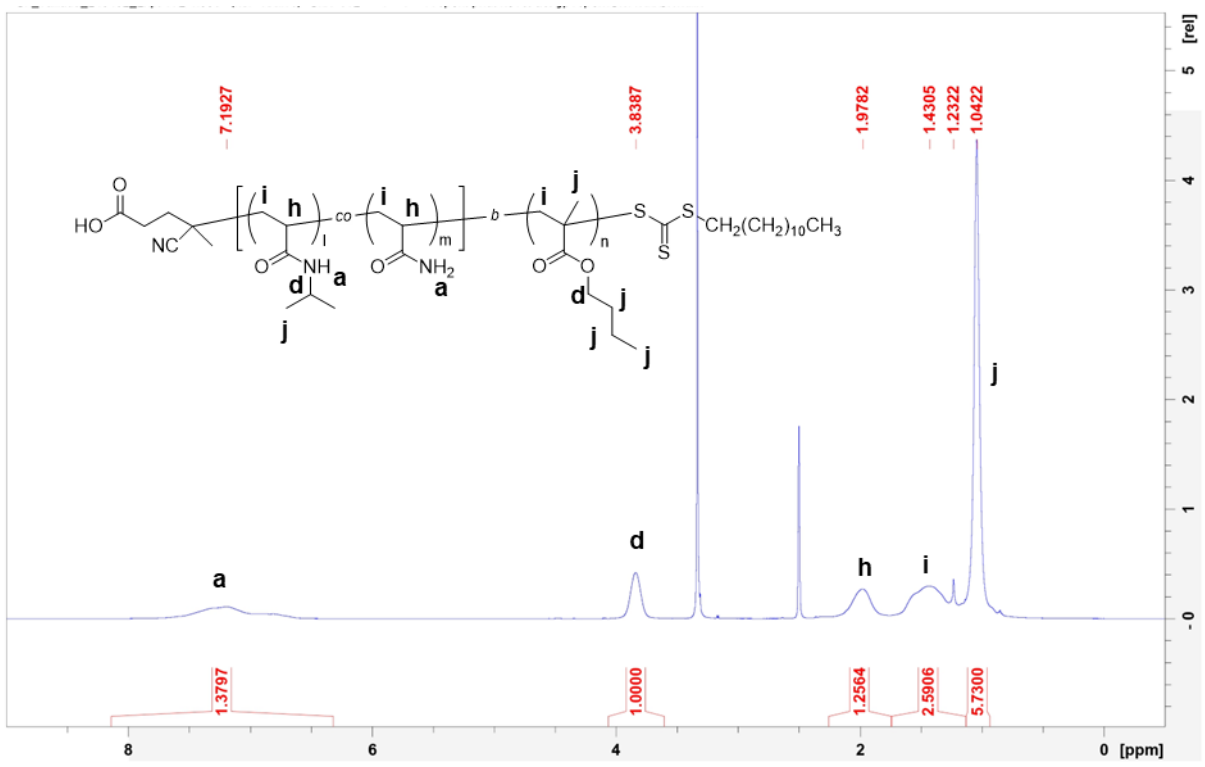

(5) DBCO-P(NIPAAm-*co*-AAm16)-*b*-PBMA in DMSO-d_6.

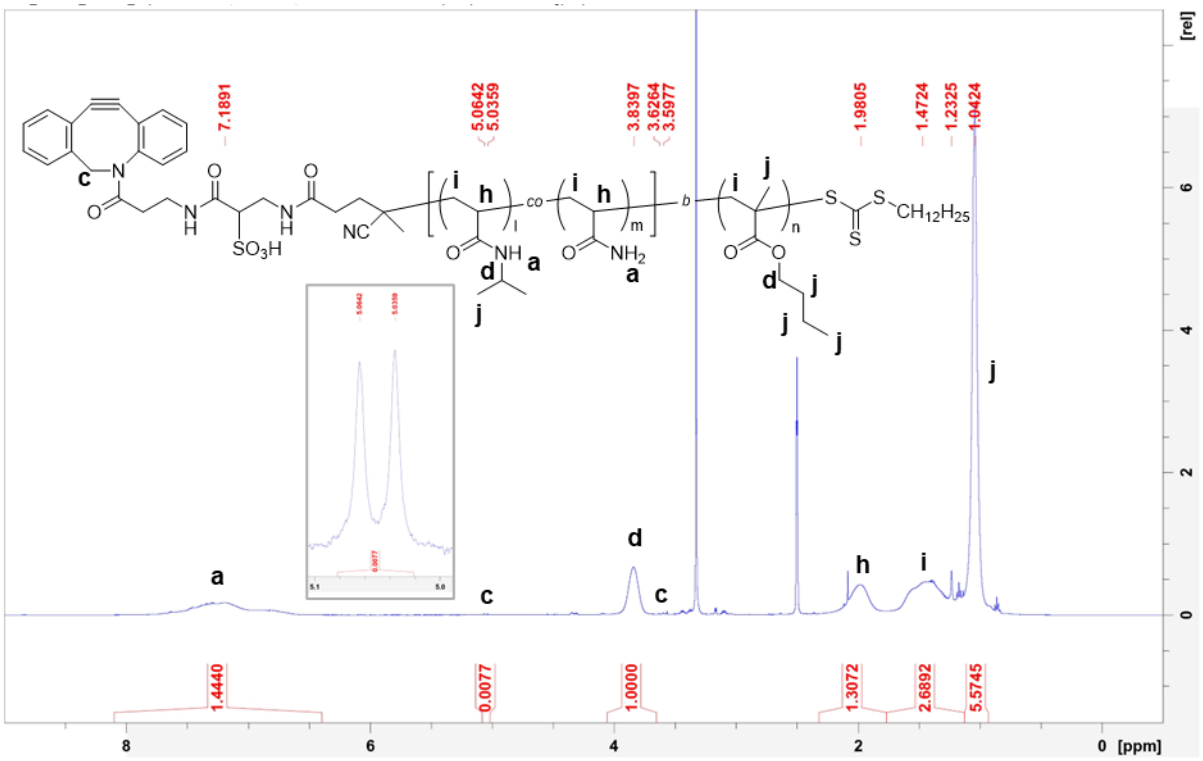

(6) P(NIPAAm-*co*-AAm16) in DMSO-d_6.

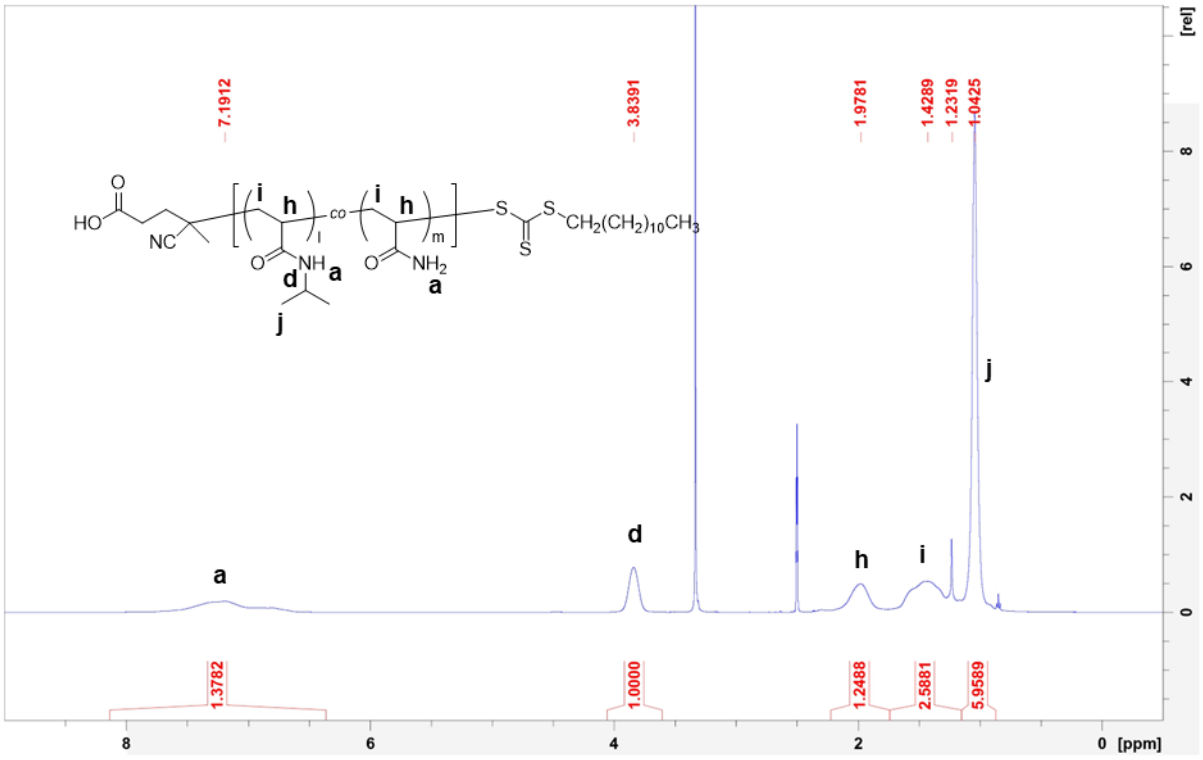

(7) P(NIPAAm-*co*-AAm16)-*b*-PBMA in DMSO-d_6.

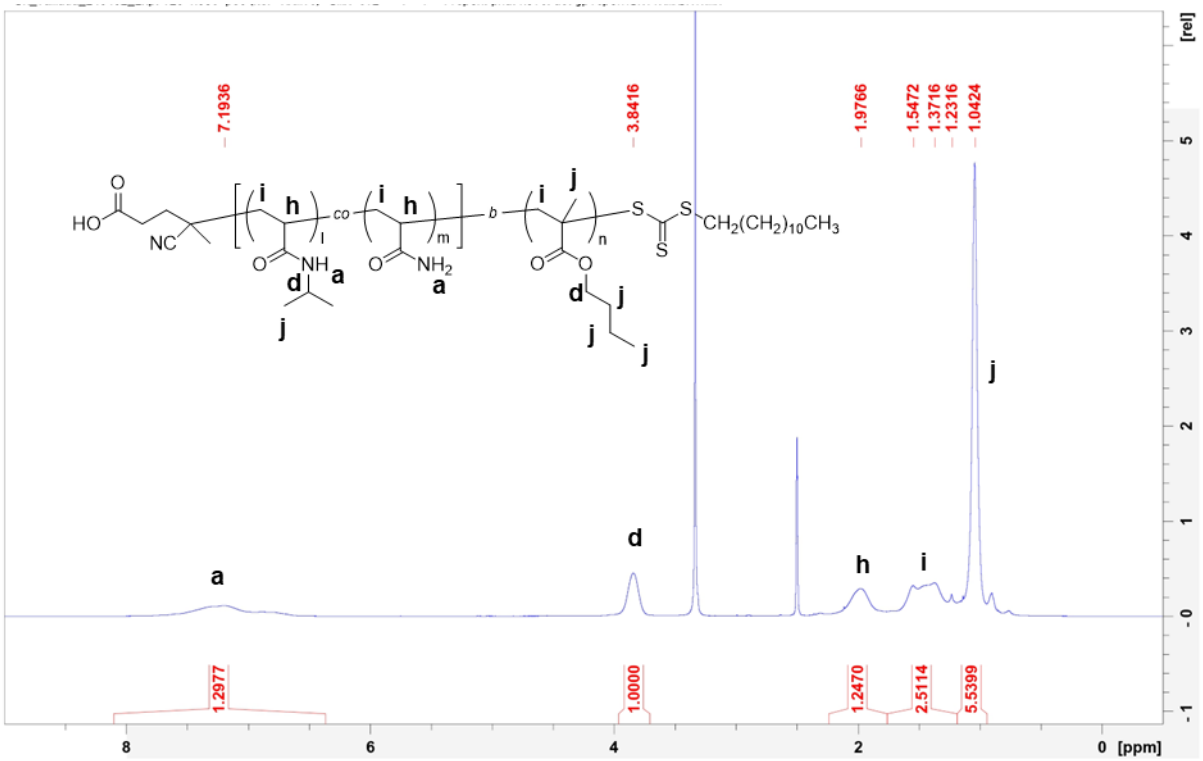

(8) P(NIPAAm-*co*-AAm8) in DMSO-d_6.

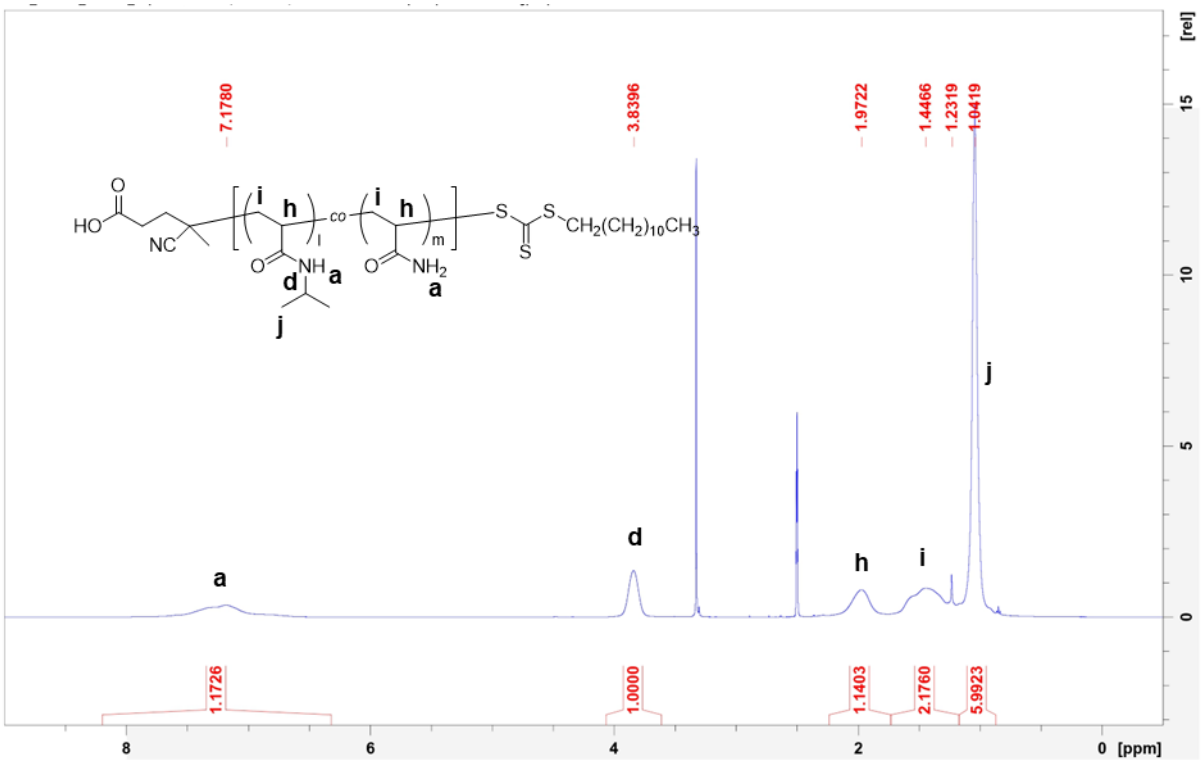

(9) P(NIPAAm-*co*-AAm8)-*b*-PBMA in DMSO-d_6.

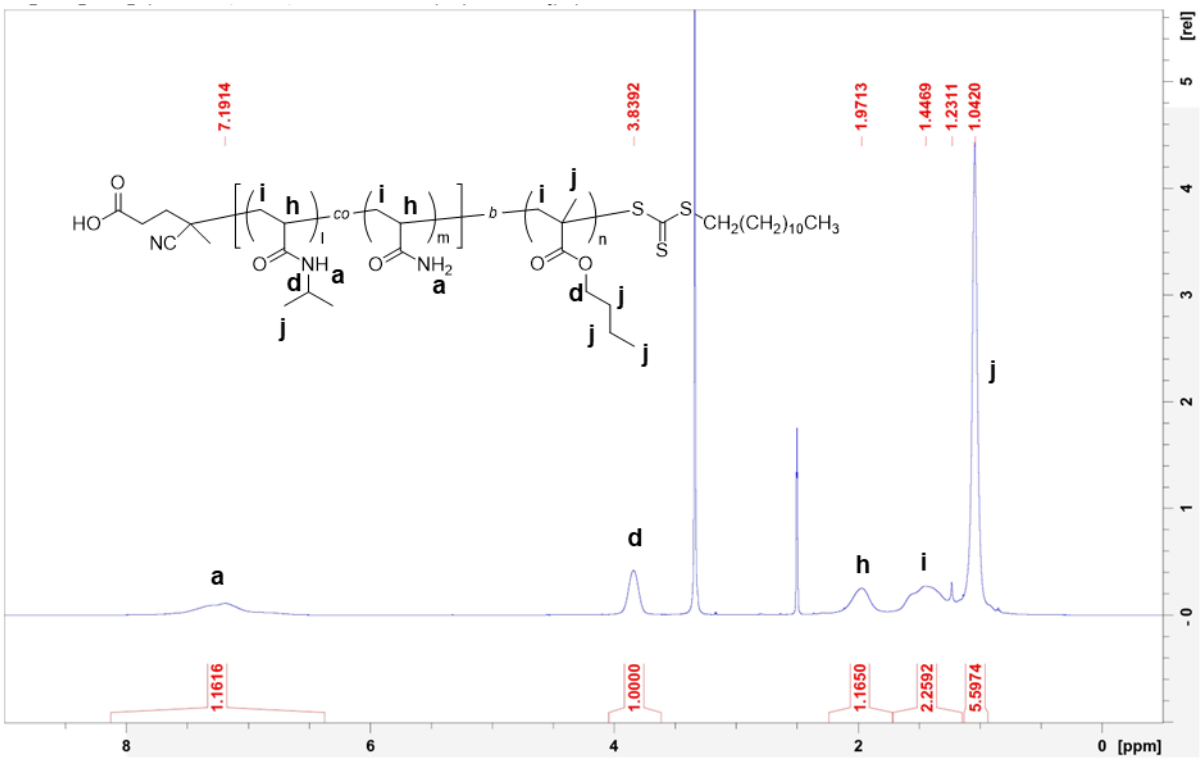

(10) P(AAm-*co*-GA) in DMSO-d_6.

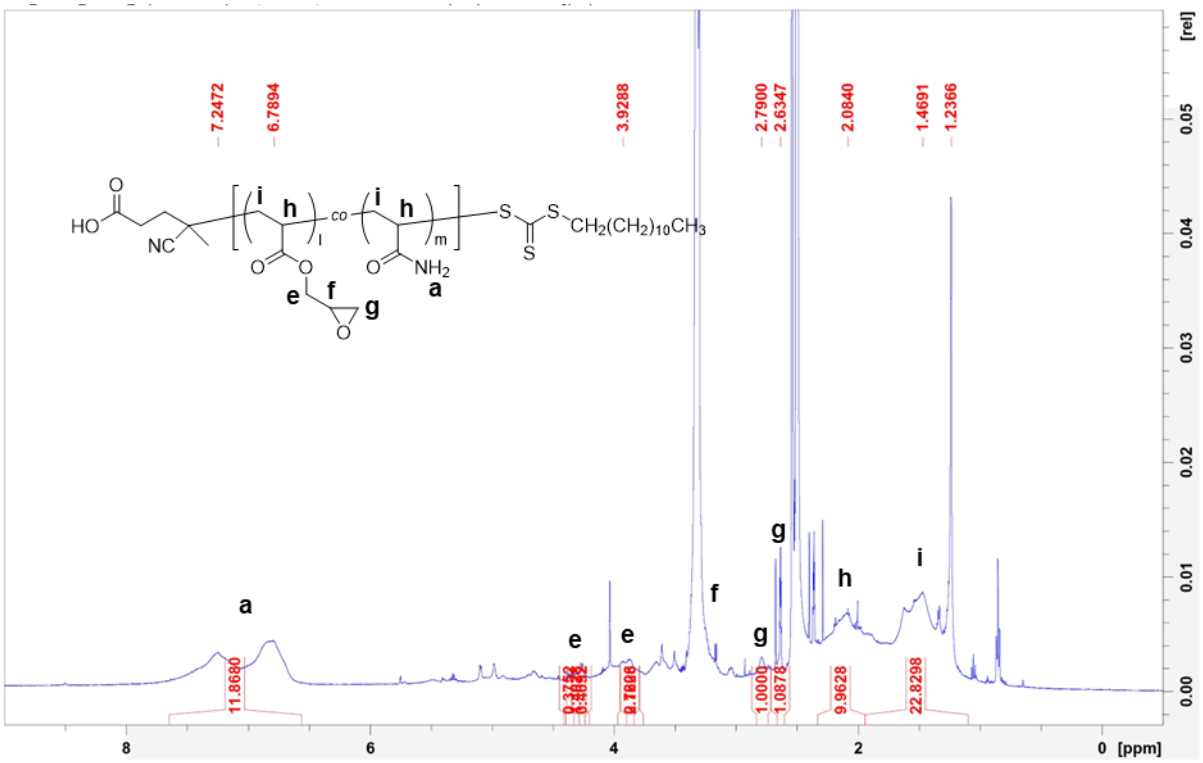

(11) P(AAm-*co*-Az)-*b*-PBMA in DMSO-d_6.

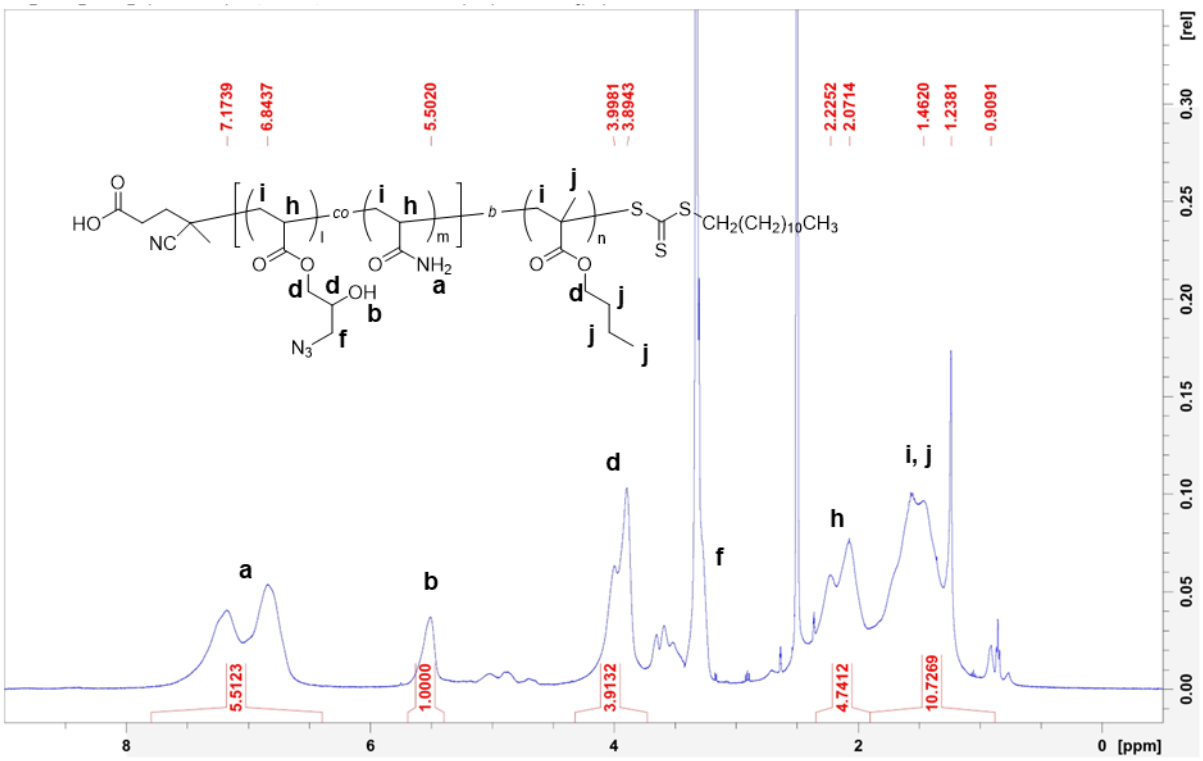

(12) P(AAm-*co*-GA)_short in DMSO-d_6.

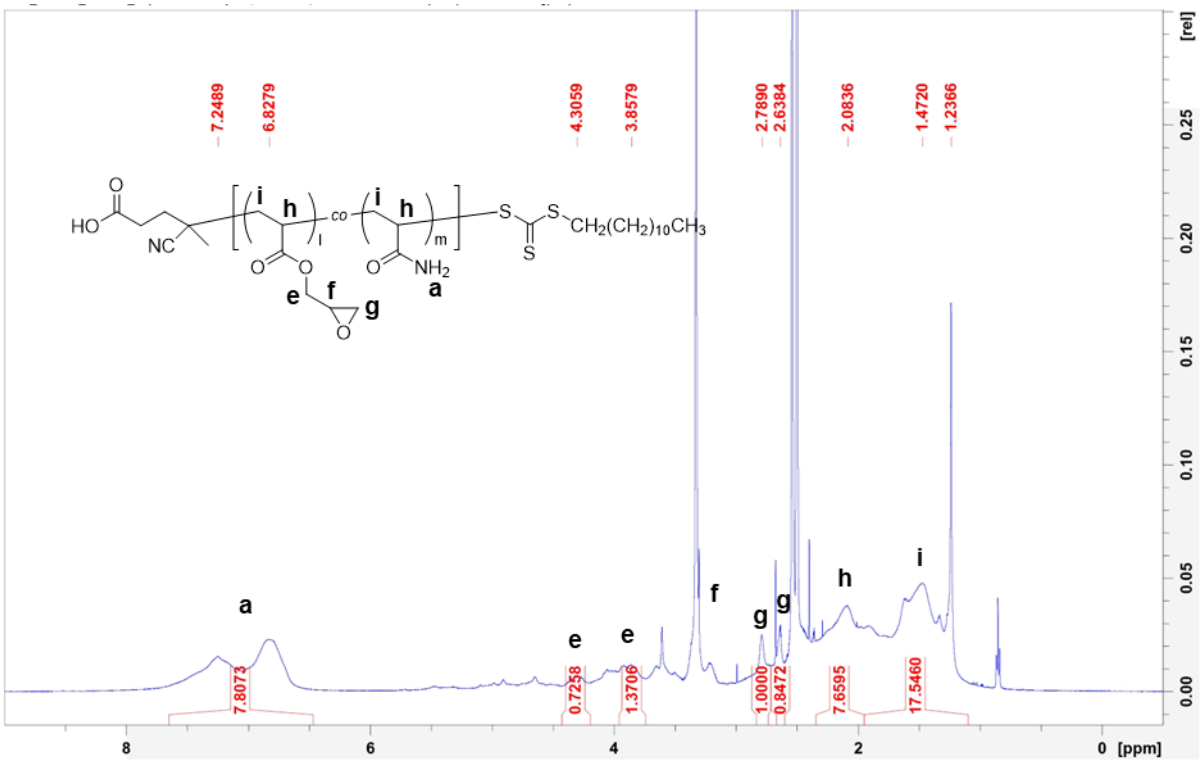

(13) P(AAm-*co*-Az)_short-*b*-PBMA in DMSO-d_6.

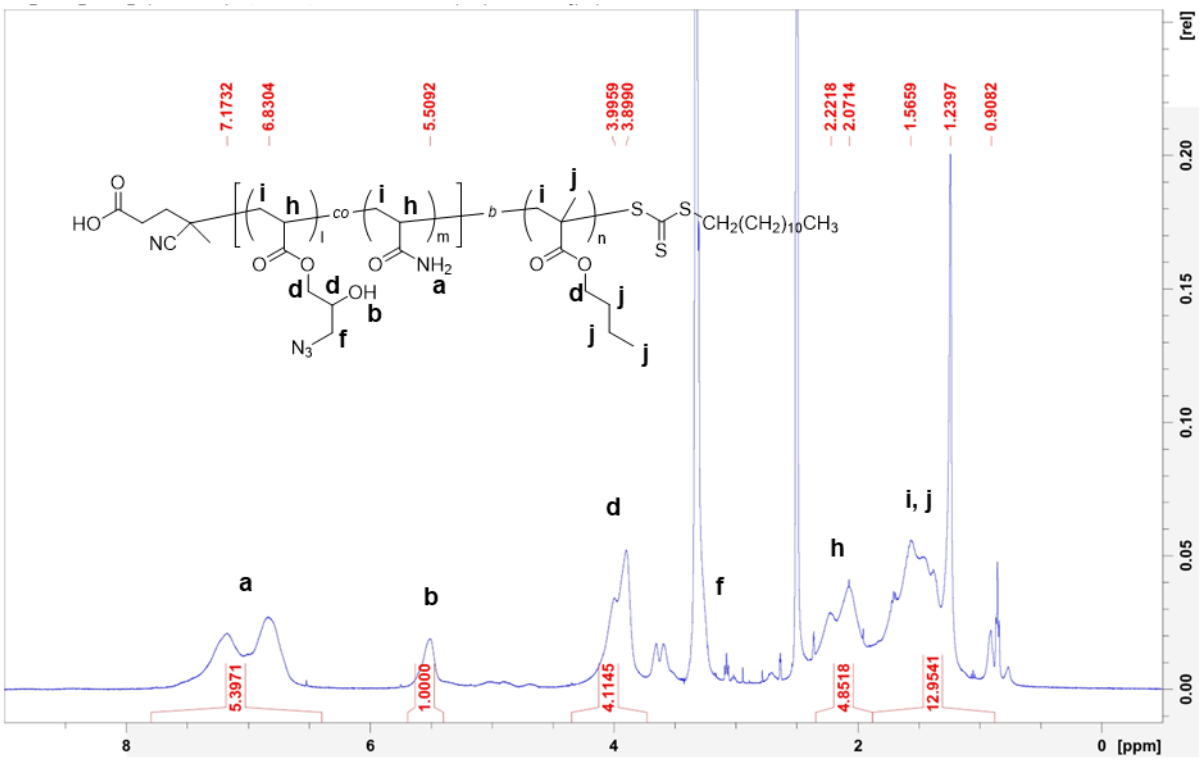

(14) P(AAm-*co*-GA)_long in DMSO-d_6.

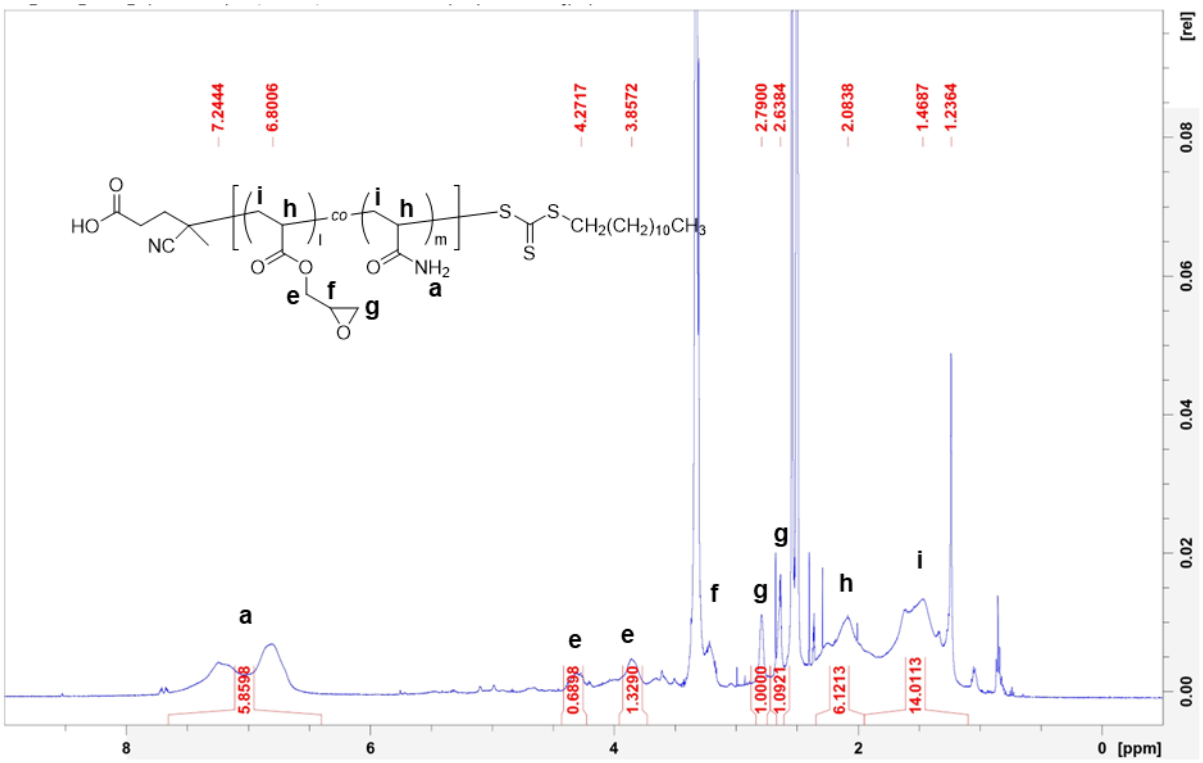

(15) P(AAm-*co*-Az)_long-*b*-PBMA in DMSO-d_6.

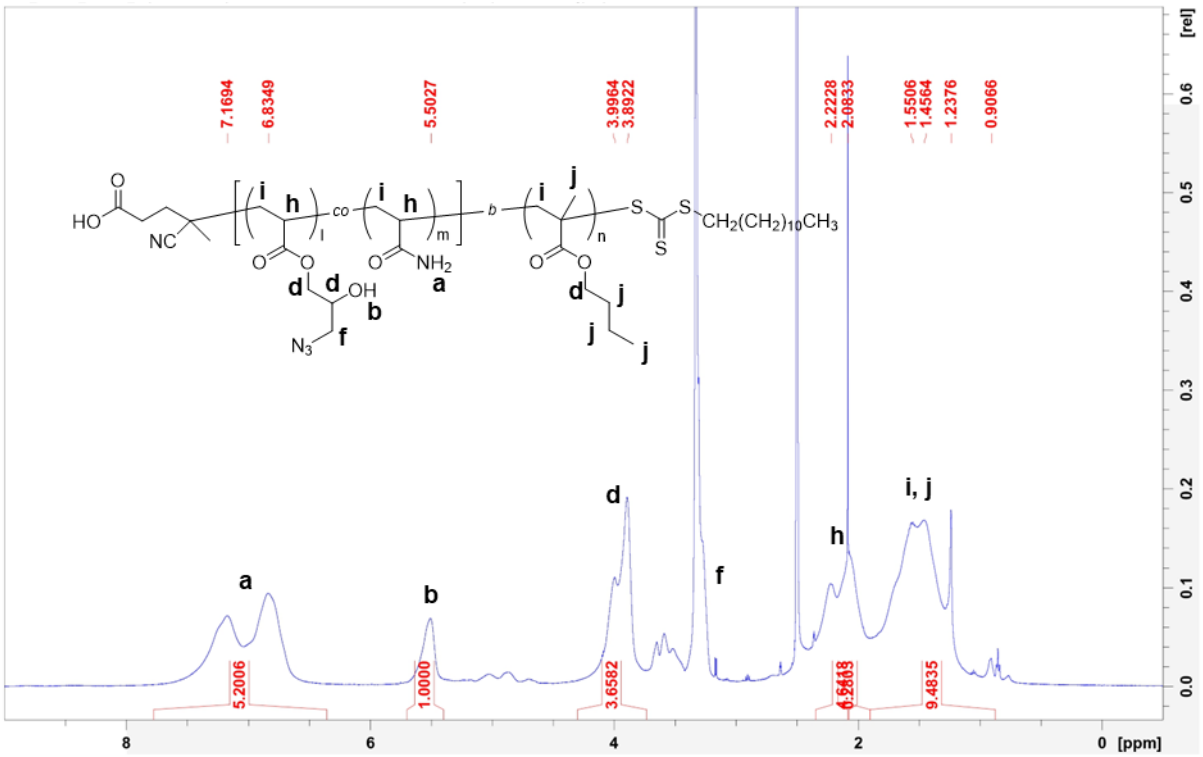

References

[SR1] Kanda, Y. Investigation of the freely-available easy-to-use software "EZR" (Easy R) for medical statistics. *Bone Marrow Transplant.* **2013**, 48(3), 452-8. https://doi.org/10.1038/bmt.2012.244.